



Providing Choice & Value

Generic CT and MRI Contrast Agents

**FRESENIUS
KABI**

CONTACT REP

AJNR

High-b-value Diffusion-weighted MR Imaging of Suspected Brain Infarction

Joel R. Meyer, Arturo Gutierrez, Bryan Mock, Delon Hebron, Jordan M. Prager, Michael T. Gorey and Daniel Homer

AJNR Am J Neuroradiol 2000, 21 (10) 1821-1829

<http://www.ajnr.org/content/21/10/1821>

This information is current as of July 28, 2025.

High-b-value Diffusion-weighted MR Imaging of Suspected Brain Infarction

Joel R. Meyer, Arturo Gutierrez, Bryan Mock, Delon Hebron, Jordan M. Prager, Michael T. Gorey, and Daniel Homer

BACKGROUND AND PURPOSE: Recent technological advances in MR instrumentation allow acquisition of whole-brain diffusion-weighted MR scans to be obtained with b values greater than 1000. Our purpose was to determine whether high-b-value diffusion-weighted MR imaging improved contrast and detection of signal changes in acute and chronic brain infarction.

METHODS: We prospectively evaluated the MR scans of 30 subjects with a history of possible brain infarction on a 1.5-T MR imager with 40 mT/meter gradients (slew rate 150 T/m/s) by use of the following single-shot echo-planar diffusion-weighted MR sequences: 1) 7999/71.4/1 (TR/TE/excitations, b = 1000; 2) 999/88.1/3, b = 2500; and 3) 7999/92.1/4, b = 3000. Diffusion-weighted MR imaging was performed in three orthogonal directions during all sequences. All subjects were scanned with fast fluid-attenuated inversion recovery (FLAIR) (10,006/145/2200/1 [TR/TE/TI/excitations]) and fast spin-echo T2-weighted (3650/95/3 [TR/TE/excitations], echo train length, 8). The diagnosis of brain infarction was established by clinical criteria.

RESULTS: Twenty women and 10 men with a mean age of 67.7 years were enrolled in the study. One subject was excluded owing to poor image quality. Twelve of 29 subjects had a clinical diagnosis of acute infarction. All 12 had lesions that were hyperintense on diffusion-weighted images at all three b values; five were cortical and seven subcortical. There was increased contrast of all lesions on high-b-value scans (b = 2500 and 3000). Lesions that were hypointense on diffusion-weighted images were identified and evaluated at the three different b values. At b = 1000, there were 19 hypointense lesions, whereas at b = 2500 and 3000 there were 48 and 55 lesions, respectively. On FLAIR and T2-weighted images, these low-signal lesions were predominantly chronic, subcortical, ischemic lesions and lacunar infarcts, but four chronic cortical infarcts, one porencephalic cyst, and one primary brain tumor were also found. Low-signal lesions were also noted to have increased contrast on high-b-value diffusion-weighted scans.

CONCLUSION: High-b-value diffusion-weighted MR imaging (b = 2500 or b = 3000) had no impact on diagnosis of acute infarction. High-b-value diffusion-weighted MR imaging (b = 2500) combined with diffusion-weighted MR imaging at b = 1000 improves tissue characterization by increasing the spectrum of observed imaging abnormalities in patients with suspected brain infarction.

Diffusion-weighted MR imaging has been shown to be highly sensitive for the diagnosis of cerebral infarction (1). Areas of cerebral infarction have de-

creased apparent diffusion, which results in increased signal intensity on diffusion-weighted MR scans. Although there is some controversy as to the exact mechanism responsible for signal changes on diffusion-weighted scans, evidence suggests that increased signal on diffusion-weighted scans is related to impeded diffusion of water as it shifts between the extracellular and intracellular compartments. In acute infarction, this is thought to be secondary to cytotoxic edema, which may reflect damage to neuronal adenosine diphosphate-dependent homeostasis (2–5). Whereas conventional MR imaging may reveal positive findings within 8 to

Received April 22, 1999; accepted after revision May 10, 2000.

From the Departments of Radiology (J.R.M., A.G., D.H., J.M.P., M.T.G.) and Neurology (J.R.M., D.H.), Northwestern University Medical School, Evanston, IL, and GE Medical Systems (B.M.), Milwaukee, WI.

Address reprint requests to Joel R. Meyer, M.D., Department of Radiology, Evanston Northwestern Healthcare, 2650 Ridge Ave., Evanston, IL 60201.

© American Society of Neuroradiology

TABLE 1: Hyperintense lesions

	b1000	b2500	b3000
# subjects	12	12	12
# lesions	16	16	16
Avg contrast ratio*	0.33	0.51 \ddot{U}	0.56 \acute{a}
Standard deviation	0.10	0.10	0.11

* Ratio defined as $(SI_I - SI_{II})/(SI_I + SI_{II})$ —see methods for explanation.

\ddot{U} denotes statistical significance ($\alpha < 0.001$).

\acute{a} denotes statistical significance ($\alpha < 0.001$).

TABLE 2: Mean ADC of acute infarcts and normal tissue

b Value	Mean ADC Infarct ($\times 10^{-4}$)	Mean ADC Contralateral NL ($\times 10^{-4}$)
1000	4.4 ± 1.3	9.0 ± 1.2
2500	3.3 ± 1.2	6.7 ± 0.7
3000	3.0 ± 0.9	6.1 ± 0.83

TABLE 3: Hypointense lesions

	b1000	b2500	b3000
Total number of lesions	19	48	55
Avg number/subject	0.66	1.67 \ddot{U}	1.90 \acute{a}
Standard deviation	1.11	2.09	2.12
Avg contrast ratio*	-0.17	-0.40 $\#$	-0.39 ∞
Standard deviation	0.20	0.19	0.17

Note.—Ratio defined as $(SI_I - SI_{II})/(SI_I + SI_{II})$, \ddot{U} Statistical significance ($\alpha = 0.03$), \acute{a} Statistical significance ($\alpha = 0.01$).

$\#$ Statistical significance ($\alpha = 0.03$), ∞ Statistical significance ($\alpha = 0.02$).

12 hours of onset of acute infarction (6–7), diffusion-weighted scans may be positive within minutes of onset in several animal models of infarction (8–11), and is more sensitive than is conventional MR imaging pulse sequences for early detection of cerebral infarction in humans (1, 12–19). Investigators have shown increased sensitivity of diffusion-weighted imaging for detection of hyperacute infarction within the first 6 hours of onset (1, 17); others have shown diffusion-weighted imaging to be valuable in detecting the subacute and chronic stages of infarction (16, 18–20).

With enhanced gradients, echo-planar diffusion-weighted imaging is rapidly becoming a standard for imaging brain infarction. Multislice whole-brain diffusion-weighted examinations can be obtained in three orthogonal planes within seconds (13). The degree of diffusion weighting of these scans correlates with the strength of the diffusion gradients applied during the acquisition. Diffusion-weighted scans are characterized by the b value (in s/mm^2), which is a function of diffusion gradient strength (G, typical $G = 20$ – 25 mT/m), the duration of the gradient (δ), and the interval between diffusion gradients (Δ) (21). Previous animal studies

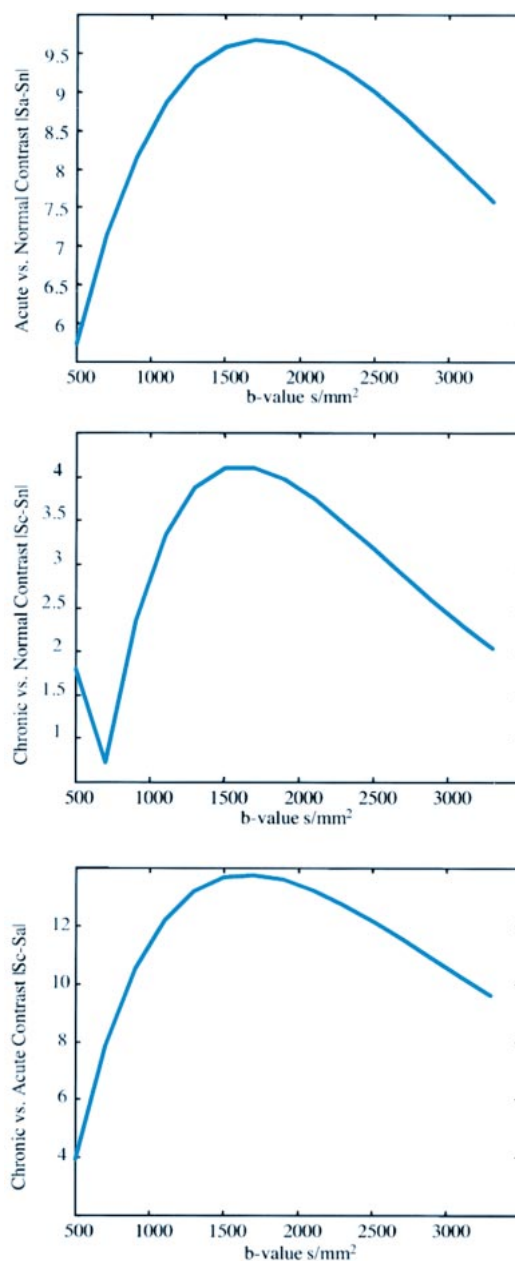


FIG 1. The signal intensity difference between three tissue types (normal gray matter tissue [assumed $ADC = 0.8 \times 10^{-3} mm^2/s$, $T_2 = 100$ ms], acute ischemic tissue [decreased $ADC = 0.4 \times 10^{-3} mm^2/s$, $T_2 = 100$ ms], and chronic lesions [elevated $ADC = 1.3 \times 10^{-3} mm^2/s$, elevated $T_2 = 100$ ms]) plotted as a function of the b value. In addition to the ADC and T_2 assumptions for each tissue, the tissue T_1 s were assumed to be equal (1000 ms) and significantly smaller than the imaging TR (10 s) such that T_1 effects could be ignored.

A, The signal difference in normal gray matter tissue and acute lesion is shown.

B, Normal tissue signal is compared with chronic lesion signal, assuming the T_2 and ADC are elevated in the chronic lesion.

C, The relative signal difference between acute and chronic lesion signal is demonstrated. In each case, the contrast reaches a maximum in the b-value range of 1500–2000 s/mm^2 . Note, however, that the largest contrast is seen in C (acute vs chronic), suggesting that higher b values may be beneficial in delineating chronically infarcted versus acutely ischemic regions.

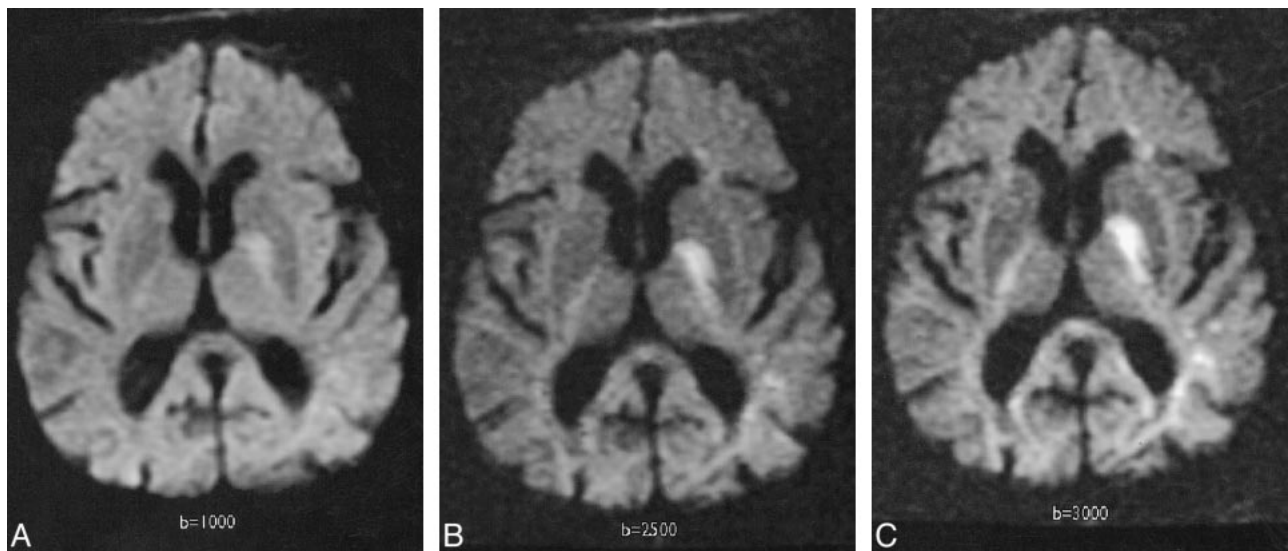


FIG 2. Trace image of hyperacute infarct in an 89-year-old woman scanned 6 hours after developing right-sided weakness and aphasia. A, Diffusion-weighted image ($b = 1000 \text{ s/mm}^2$) demonstrates a high-signal area consistent with acute infarct in the left basal ganglia and posterior limb of the internal capsule.

B, Diffusion-weighted image ($b = 2500 \text{ s/mm}^2$) demonstrates the increased contrast of the high-signal lesion.

C, Diffusion-weighted image ($b = 3000 \text{ s/mm}^2$) also demonstrates this lesion more clearly than at $b = 1000$; anisotropic effects are evident in the posterior periventricular regions.

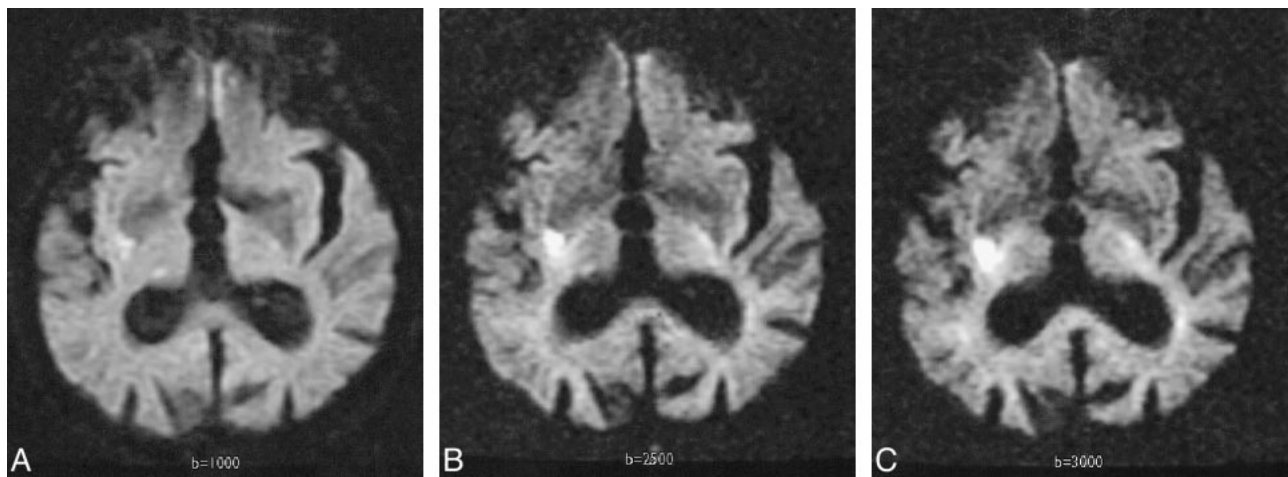


FIG 3. Acute infarct in an 82-year-old man scanned at 22 hours.

A, Diffusion-weighted image with $b = 1000 \text{ s/mm}^2$ demonstrates a high-signal area consistent with acute infarct in the right basal ganglia along the posterior lenticular nucleus. The posterior horns of the lateral ventricles are prominent.

B, Diffusion-weighted image at $b = 2500 \text{ s/mm}^2$ demonstrates the high-signal lesion with greater contrast.

C, Diffusion-weighted image at $b = 3000 \text{ s/mm}^2$ also demonstrates this lesion more clearly than at $b = 1000$; anisotropic effects are evident in the contralateral internal capsule and corona radiata.

of brain infarction have routinely used higher gradient strengths (up to 60 mT/M) to generate b values of 1400–1800 (8–9, 22–24), with one reporting a b value of 3580 (25). Most prior diffusion-weighted imaging studies of human brain infarction have been performed with b values of 1000 or less (21–26), although one reported a b value of 1463 (13). The purpose of this study was to determine the role of high- b -value ($b = 2500$ or 3000) diffusion-weighted imaging for lesion detection in acute and chronic brain infarction.

Methods

A research protocol for high- b -value diffusion-weighted MR imaging in possible brain infarction was approved by our Institutional Review Board. We conducted a prospective study of 30 consecutive patients with a clinical history of possible brain infarction who were referred to us for MR imaging of the brain. Informed consent was obtained from all subjects. MR imaging was performed on a 1.5-T MR imager with 40-mT/m gradients (G) (slew rate 150 T/m/s) by use of the following single-shot echo-planar diffusion-weighted MR sequences: 1) 7999/71.4/1 (TR/TE/excitations), $b = 1000/32 \text{ s}$; 2) 7999/88.1/3, $b = 2500/1 \text{ min } 36 \text{ s}$; 3) 7999/92.1/4, $b =$

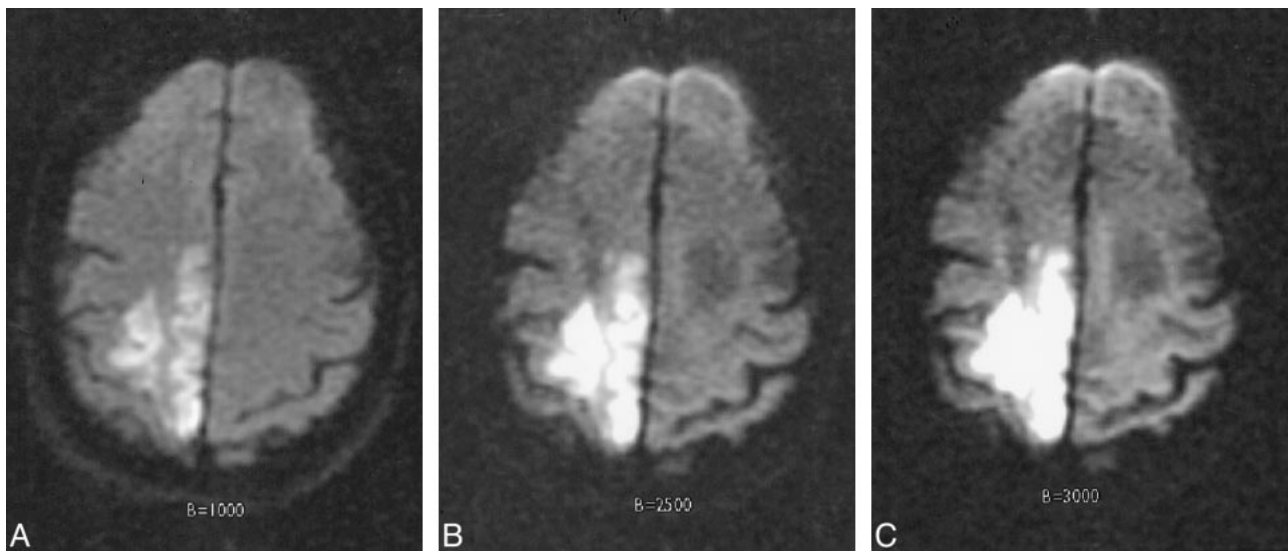


FIG 4. Acute infarct in a 94-year-old woman scanned 12 hours after developing left-sided hemiparesis.

A, Diffusion-weighted image with $b = 1000$ s/mm² demonstrates a high-signal area consistent with acute infarct in the right parietal lobe.

B, Diffusion-weighted image at $b = 2500$ s/mm² demonstrates the high-signal lesion with greater contrast.

C, Diffusion-weighted image at $b = 3000$ s/mm² also demonstrates this high-signal lesion more clearly than at $b = 1000$.

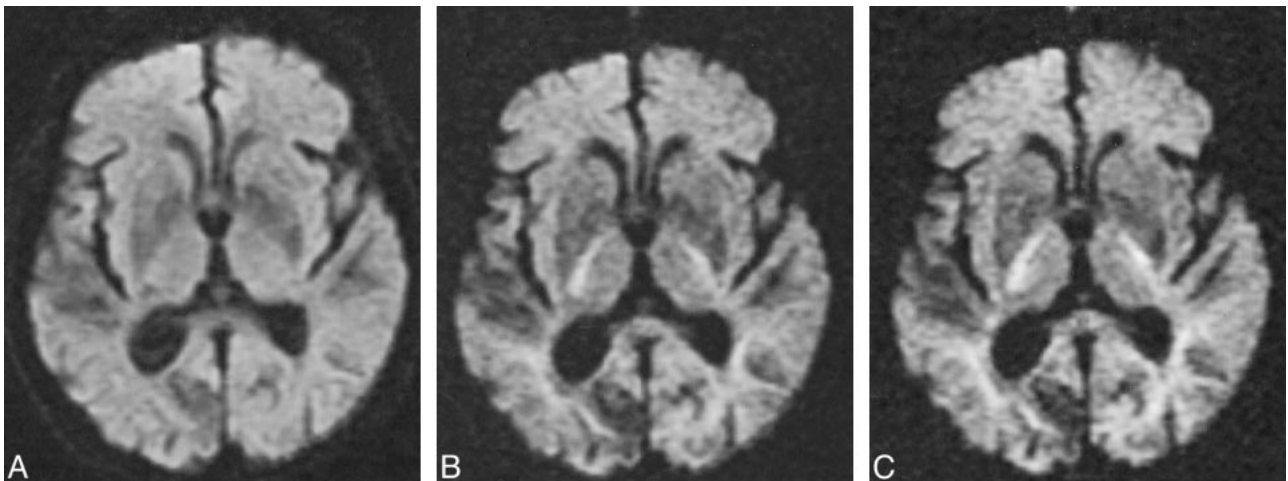


FIG 5. Transient ischemic attack and chronic infarct in a 90-year-old woman with a remote history of cerebral infarct, scanned 2 hours after developing right-sided weakness and left-sided facial droop. Her symptoms resolved spontaneously within 11 hours.

A, Diffusion-weighted image with $b = 1000$ s/mm² negative for acute infarcts, though a low-signal area of increased diffusion, consistent with chronic infarct, is noted in the right occipital lobe.

B, Diffusion-weighted image at $b = 2500$ s/mm² demonstrates the low-signal lesion with greater contrast.

C, Diffusion-weighted image at $b = 3000$ s/mm² also demonstrates this lesion more clearly than at $b = 1000$.

3000/2 min 8 s. Diffusion-weighted MR imaging was performed in three orthogonal directions during all sequences. All subjects were also scanned with fast fluid-attenuated inversion recovery (10,006/145/ 2200/1 [TR/TE/TI/excitations]) and fast spin-echo T2-weighted (3650/95/3 [TR/TE/excitations], echo train length, 8) sequences. One patient underwent proton spectroscopy and stereotactic biopsy to confirm diagnosis of primary brain tumor. The clinical diagnosis of stroke and onset of symptoms was established by clinical criteria.

Trace images using the information from the three orthogonal images were photographed and reviewed by two experienced neuroradiologists in concert and by consensus. Qualitative review included detection of low- and high-signal lesions on diffusion-weighted images at different b values. The number of lesions noted at different b values was tabulated.

Quantitative review involved calculating contrast ratios of lesions relative to background at the three b values. To quantify the contrast of lesions at different b values, a contrast ratio was defined as $SI_I - SI_{II} / SI_I + SI_{II}$, where SI_I = signal intensity at the lesion (hypo- or hyper intense), SI_{II} = signal intensity at normal brain, and signal intensity/contrast was measured at an MR workstation by use of standard software (Fig 1).

This contrast ratio, which is defined as the relative signal intensity difference in an image between two adjacent structures, was compared across identically sliced images at different b values to determine lesion contrast at different b values (27). A two-sided Student's t test was used to determine significance at .05.

An analysis of the MR signal behavior suggests that diffusion-weighted imaging with b values greater than 1000 s/mm²

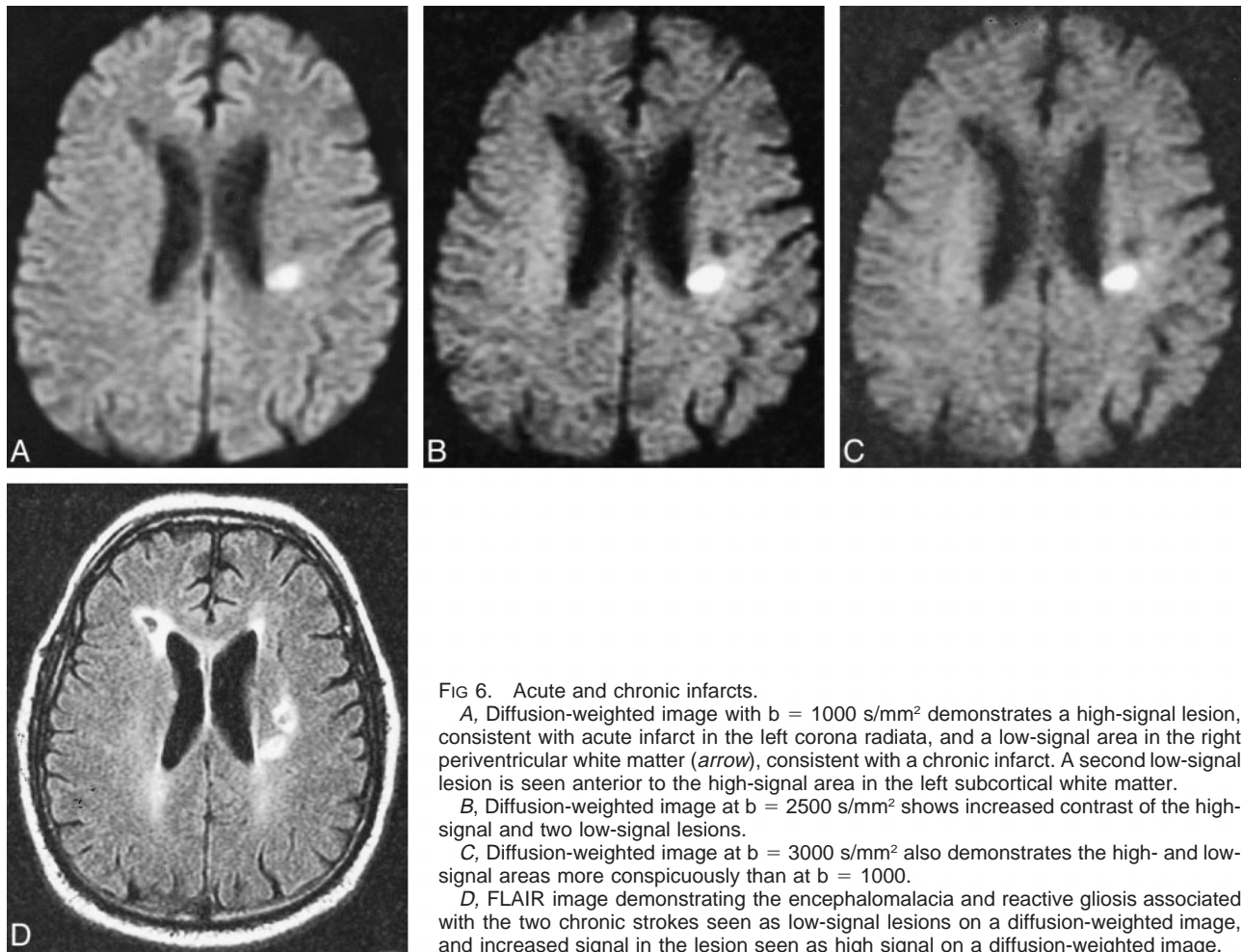


FIG 6. Acute and chronic infarcts.

A, Diffusion-weighted image with $b = 1000 \text{ s/mm}^2$ demonstrates a high-signal lesion, consistent with acute infarct in the left corona radiata, and a low-signal area in the right periventricular white matter (arrow), consistent with a chronic infarct. A second low-signal lesion is seen anterior to the high-signal area in the left subcortical white matter.

B, Diffusion-weighted image at $b = 2500 \text{ s/mm}^2$ shows increased contrast of the high-signal and two low-signal lesions.

C, Diffusion-weighted image at $b = 3000 \text{ s/mm}^2$ also demonstrates the high- and low-signal areas more conspicuously than at $b = 1000$.

D, FLAIR image demonstrating the encephalomalacia and reactive gliosis associated with the two chronic strokes seen as low-signal lesions on a diffusion-weighted image, and increased signal in the lesion seen as high signal on a diffusion-weighted image.

can improve contrast-to-noise ratio between high-signal lesions, regions of decreased diffusion, and surrounding tissue. Given two tissues, S_0 and S_1 , the contrast-to-noise ratio is given by:

$$CNR = \frac{|S_1 - S_0|}{\sigma} \quad (1)$$

where

$$S_0 = S \cdot e^{-(TE/T2_0)} \times (1 - 2 \cdot e^{-(TR-TE/2)/T1_0} + e^{-TR/T1_0}) \cdot e^{-bD_0}$$

and

$$S_1 = S \cdot e^{-(TE/T2_1)} \times (1 - 2 \cdot e^{-(TR-TE/2)/T1_1} + e^{-TR/T1_1}) \cdot e^{-bD_1}$$

Because the noise of MR imaging is proportional to the total data acquisition time, maximizing the contrast to noise in diffusion-weighted imaging amounts to maximizing the absolute signal difference $|S_1 - S_0|$.

Figure 1 demonstrates the change in signal $|S_1 - S_0|$ between three tissue types: a) normal gray matter tissue (assumed apparent diffusion coefficient [ADC] = $0.8 \times 10^{-3} \text{ mm}^2/\text{s}$, $T_2 = 100 \text{ ms}$), b) acute ischemic tissue (decreased ADC = $0.4 \times 10^{-3} \text{ mm}^2/\text{s}$, $T_2 = 100 \text{ ms}$), and c) chronic lesions (elevated ADC = $1.3 \times 10^{-3} \text{ mm}^2/\text{s}$, elevated $T_2 = 150 \text{ ms}$) as a function of the b value. In addition to the ADC and T_2 assumptions for each tissue, the tissue T_1 s were assumed to be equal (1000 ms) and significantly smaller than the imaging

TRs (10 s) such that T_1 effects could be ignored. In Figure 1A, the contrast between normal tissue and acute lesion signal is plotted. In Figure 1B, normal tissue signal is compared with chronic lesion signal, assuming the T_2 and ADC are elevated in the chronic lesion. In Figure 1C, the relative signal difference between acute and chronic lesion signal is shown. In each case, the contrast reaches a maximum in the b -value range of 1500–2000 s/mm^2 . Note, however, that the largest difference is seen in Figure 1C (acute vs chronic), suggesting that higher b values may be beneficial in delineating chronically infarcted versus acutely ischemic regions.

ADC calculations were performed on all subjects with acute infarcts at each b value. ADC measurements were also derived from contralateral normal brain at each b value. Mean ADCs were calculated and compared.

Results

Twenty women and 10 men with a mean age of 67.7 years were enrolled in the study. One patient was dropped from the study owing to excessive motion artifact on all scans. Presenting symptoms included hemiparesis, numbness, facial droop, slurred speech, aphasia, blurred vision, mental status changes, diplopia, seizure, and otalgia. The timing of MR scanning relative to symptom onset was less than 24 hours in eight subjects, within 24 to 48 hours in 10, and between 48 hours and 14 days in 11.

A clinical diagnosis of acute infarction was established in 12 of 29 subjects. All 12 had hyperintense lesions on diffusion-weighted images at all three b values, five of which were cortical and seven subcortical, including a hemorrhagic lacunar infarct with mixed signal on the diffusion-weighted image. No subject had a recent infarction involving the brain stem. All high-signal lesions on diffusion-weighted images showed improved lesion contrast at higher b values (Figs 2 and 3). The average contrast ratios for hyperintense lesions are summarized in Table 1.

One additional subject had a hyperintense lesion on diffusion-weighted images at all b values, with a clinical diagnosis of transient ischemic attack. This appeared as a mixed-signal lesion with central low signal and peripheral high signal. A diffusion-weighted study performed 5 weeks prior to the high-b-value examination confirmed that this lesion was an evolving infarct rather than an acute event.

Mean ADC values for acute infarcts and contralateral normal brain are presented in Table 2.

Low-signal lesions were predominantly subcortical ischemic and lacunar infarcts, but three chronic cortical infarcts, one 5-week-old evolving infarct, one porencephalic cyst, and one primary brain tumor were found. Qualitatively, the low-signal lesions were more conspicuous at higher b values (Figs 4–7), leading to a greater number of lesions recorded at higher b values: 19 at b = 1000, 48 at b = 2500, and 55 at b = 3000. The contrast ratios of low-signal-intensity lesions are summarized in Table 3. In one subject, a large area of low signal was demonstrated at b = 2500/3000, which was not shown at b = 1000. This subject underwent MR spectroscopy and subsequent stereotactic brain biopsy, confirming the diagnosis of oligoastrocytoma (Fig 7).

Discussion

Diffusion-weighted MR imaging has dramatically improved our ability to diagnose cerebral infarction. Whereas conventional MR images may be normal within the first 8 to 12 hours, diffusion-weighted MR images may be positive minutes after onset of infarction (8–11). Clinical experience with diffusion-weighted imaging within the first 6 hours of infarction revealed a sensitivity of 94% and specificity of 100% for diagnosis of acute infarction (1). Other investigators have shown the importance of diffusion-weighted scans in the diagnosis of subacute and chronic infarction (16). Although early investigators used spin-echo and navigated spin-echo techniques to obtain diffusion-weighted scans, with the improvement of MR gradient technology, echo-planar imaging is rapidly becoming the standard for rapid whole-brain diffusion-weighted imaging. More recently, whole-brain diffusion-weighted scans with b values up to 3000 can be acquired, without requiring a significantly longer gradient duration or gradient interval,

thereby eliminating the need for prolonged echo times.

Prior diffusion-weighted imaging studies have used b values ranging from 500 to 1463. One study indicated that higher b values (b = 1463) improved the sensitivity of diffusion-weighted imaging for detection of the smallest areas of infarction (13). Our study extends this work by assessing the utility of high b values in brain infarction. Whereas prior studies focused on the evaluation of high-signal-intensity lesions associated with acute infarction, our study evaluated both high- and low-signal-intensity lesions (areas of decreased and increased diffusion). Our study showed a statistically significant increase in the contrast ratio of high-signal-intensity lesions at b = 2500 and b = 3000 versus b = 1000. Although no additional lesions were documented at higher b values, the increased conspicuity of these lesions suggests that high-b-value diffusion-weighted imaging may facilitate interpretation of acute infarction, particularly with smaller lesions, as others have suggested. Comparing b = 2500 to b = 3000, there was no significant improvement in the contrast ratios. Furthermore, at b = 3000, the decrease in signal to noise required additional signal averages, which prolonged the examination time by approximately 90 seconds.

ADC calculations were consistent with the improved contrast ratios of high signal lesions on diffusion-weighted images at different b values. At higher b values, the observed ADCs were lower for both contralateral normal tissue as well as areas of acute infarction. Other investigators confirm the observation that the relationship between ADC and b-value changes with increasing b values (personal communication, Gregory A. Sorenson). The ADC measurements performed on our data were two-point ADC measurements between no diffusion weighting (T2 image, b value = 0) and the diffusion-weighted image. Because two-point ADC measurements represent a single aggregate diffusion value within a region, such measurements cannot accurately represent differences in diffusion from different compartments. The combination of MR imaging's partial volume effects and the recently observed multiexponential behavior of diffusion attributed to extracellular (fast diffusion) and intracellular (slow diffusion) compartments (28), might render two-point ADC calculations inappropriate when combined with high-b-value imaging. Nevertheless, high-b-value diffusion-weighted imaging improves the gray-white matter differentiation on ADC maps and may improve the visual assessment of areas of decreased diffusion.

The ability to assess and document low-signal-intensity lesions visually was significantly improved with high b values. Detection of low-signal lesions increased and contrast ratios improved with high b values. Although it is generally agreed that chronic infarcts are characterized by increased diffusion of water, the ability of diffusion-weighted imaging to detect these lesions reliably has been

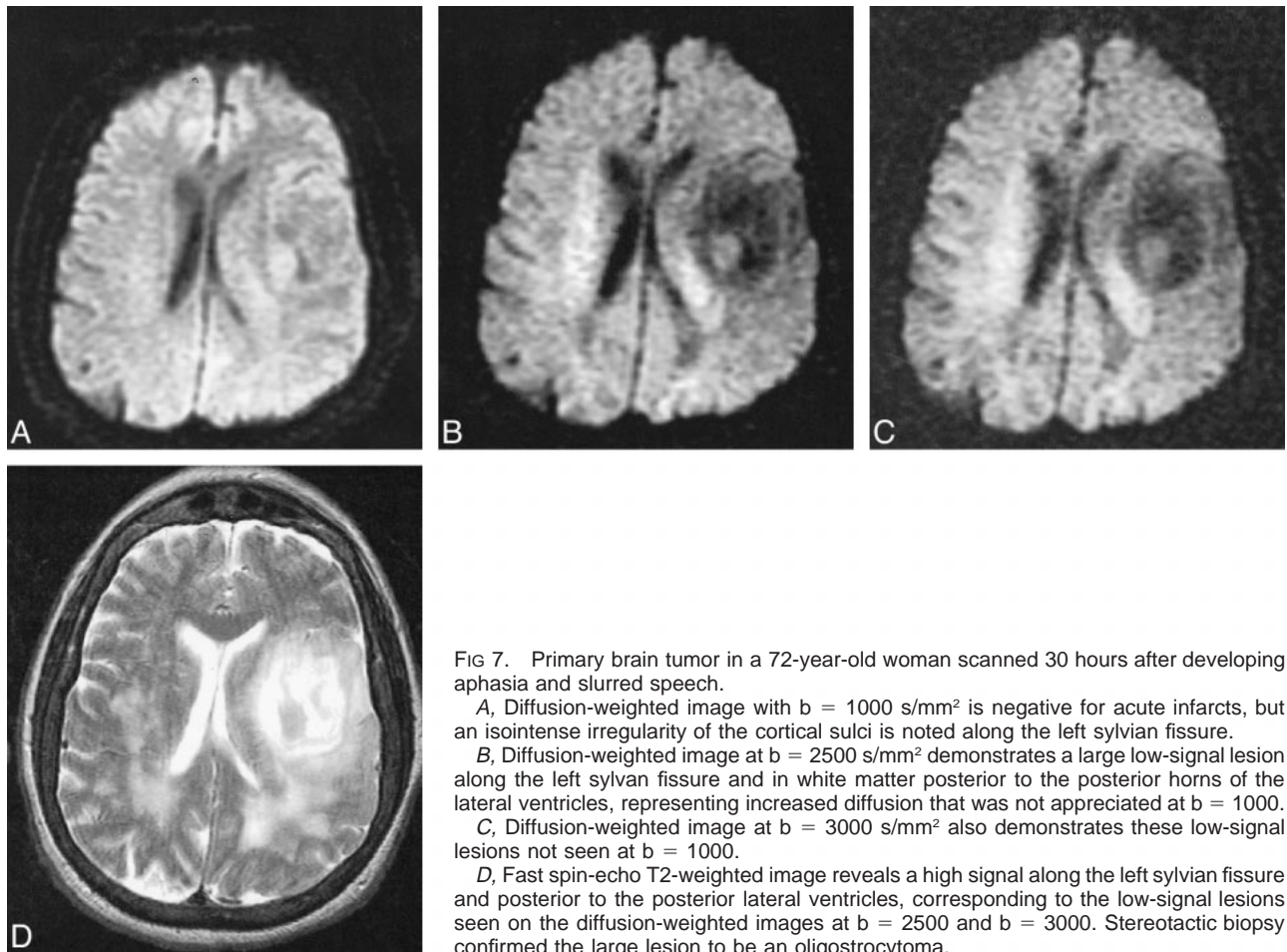


FIG 7. Primary brain tumor in a 72-year-old woman scanned 30 hours after developing aphasia and slurred speech.

A, Diffusion-weighted image with $b = 1000 \text{ s/mm}^2$ is negative for acute infarcts, but an isointense irregularity of the cortical sulci is noted along the left sylvian fissure.

B, Diffusion-weighted image at $b = 2500 \text{ s/mm}^2$ demonstrates a large low-signal lesion along the left sylvian fissure and in white matter posterior to the posterior horns of the lateral ventricles, representing increased diffusion that was not appreciated at $b = 1000$.

C, Diffusion-weighted image at $b = 3000 \text{ s/mm}^2$ also demonstrates these low-signal lesions not seen at $b = 1000$.

D, Fast spin-echo T2-weighted image reveals a high signal along the left sylvian fissure and posterior to the posterior lateral ventricles, corresponding to the low-signal lesions seen on the diffusion-weighted images at $b = 2500$ and $b = 3000$. Stereotactic biopsy confirmed the large lesion to be an oligodendroglioma.

limited. This may in part relate to so-called T2 shine-through effect, which may cancel low signal from chronic infarcts with increased diffusion. (20, 21). We hypothesize that more heavily diffusion-weighted images are less sensitive to T2 signal alterations (T2 shine-through), thereby improving imaging of chronic infarcts as well as entities with increased diffusion such as cysts, brain tumors, and brain edema. Our case of a primary brain tumor, which only demonstrated low signal at higher b values, illustrates the potential value of this technique (Fig 7). Others have shown that diffusion-weighted imaging with b values less than 1000 s/mm^2 can distinguish areas of nonenhancing tumor from areas of peritumoral edema, both of which appear nonenhancing on T1- and bright on T2-weighted images of gliomas (29). This study also suggested advantages of diffusion-weighted imaging with $b = 777$ over $b = 215$. Others have demonstrated the utility of diffusion-weighted imaging in differentiating extraaxial cysts from epidermoid tumors (30) and differentiating brain cystic abscesses filled with paramagnetic protein from solid masses (31). High- b -value diffusion-weighted images, therefore, offer a potentially valuable complement to conventional MR imaging techniques for studying chronic processes and complex lesions.

There are some limitations to high- b -value diffusion-weighted imaging. High- b -value diffusion-weighted imaging requires a hardware upgrade, because most scanners are not capable of generating a 40-mT/m gradient field. This would otherwise require an increased gradient duration and interval, with an accompanying increase in echo time, all of which degrade image quality. Secondly, high- b -value diffusion-weighted scans have accentuated anisotropic effects in the brain stem and posterior capsular regions. This might limit the utility of high- b -value diffusion-weighted imaging in the brain stem as well as other areas where white matter tracts are prominent (Figure 3). Although this was not a limitation in this study, further investigation would be necessary to determine which b value is best for evaluation of brain stem infarctions. Finally, high- b -value diffusion-weighted imaging requires longer scanning times. Multiple excitations are needed to overcome signal-to-noise problems at high b values, thereby increasing imaging time from 32 seconds ($b = 1000$) to 2 minutes and 8 seconds ($b = 3000$).

A fundamental question not addressed in this study is whether increased b -value diffusion-weighted imaging could allow detection of ischemic but not infarcted tissue. Although reversible

diffusion changes have been reported at lower b values, most commonly a high signal abnormality on the diffusion-weighted image indicates infarcted tissue (19, 21). This would require a study that involved high-b-value serial scanning to determine reversibility. A related unanswered question is how higher b values affect the observed time course of stroke. Serial high-b-value diffusion-weighted scans may help address this important issue.

Finally, it is unclear whether high-b-value diffusion-weighted imaging solves the problem of T2 shine-through, thereby eliminating the need to produce ADC maps. ADC maps address the issue of T2 shine and offer the advantage of allowing ready differentiation of acute from chronic infarcts (25). Imaging at higher b-values might not alter these findings at all, because ADC maps that are constructed should theoretically be independent of the b value. Further investigation and comparison of ADC maps with high-b-value diffusion-weighted images would be helpful to answer this question.

Despite improved contrast of high-signal lesions, high-b-value diffusion-weighted imaging did not improve our ability to diagnose acute infarction in patients with suspected infarction. An increased spectrum of imaging abnormalities was observed at higher b values, including improved contrast and increased detection of low-signal-intensity lesions. The improved detection of low-signal lesions results in better visual characterization of brain lesions with diffusion-weighted imaging. As opposed to a "light bulb" test that only answers the question of whether a recent infarct is present, high-b-value diffusion-weighted imaging offers more specific tissue characterization of brain lesions. Although this study addresses applications in brain infarction, better visual assessment of low- and high-signal lesions may have significant applications in other neurologic disorders. The combination of low- and high-b-value diffusion-weighted acquisitions may prove to be efficacious in a variety of brain diseases.

Conclusion

High-b-value diffusion-weighted imaging provides improved tissue characterization with better visualization of acute and chronic infarction. Although the improved contrast of high-signal lesions with high b values did not demonstrate additional areas of acute infarction, obtaining two b values ($b = 1000$ and $b = 2500$) resulted in improved detection of low-signal lesions (chronic infarction and brain tumor). No further improvement in lesion conspicuity was demonstrated at $b = 3000$.

References

1. Lovblad KO, Laubach HJ, Baird AE, et al. **Clinical experience with diffusion-weighted MR in patients with acute stroke.** *AJNR Am J Neuroradiol* 1998;19:1061-1066
2. Benveniste H, Johnson GA. **Mechanisms of ischemia-induced changes in brain water diffusion coefficient studied by brain MRI and brain microdialysis.** *Stroke* 1992;23:746-754
3. Baker LL, Kucharczyk J, Sevick RJ, Mintorovich J, Moseley M. **Recent advances in MR imaging/spectroscopy of cerebral ischemia.** *AJR Am J Roentgenol* 1991; 156:1133-1143
4. Sevick RJ, Kanda F, Mintorovich J, et al. **Cytotoxic brain edema: assessment with diffusion-weighted MR imaging.** *Radiology* 1992;185:687-690
5. Mintorovich J, Baker LL, Yang GY, et al. **Diffusion weighted hyperintensity in early cerebral ischemia: correlation with brain water content and ATPase activity.** *Proc Soc Magn Reson* 1991;10:329
6. Bryan RN, Levy LM, Whitlow WD, Killian JM, Preziosi TJ, Rosario JA. **Diagnosis of acute cerebral infarction: comparison of CT and MR imaging.** *AJNR Am J Neuroradiol* 1991;12:611-620
7. Yuh WT, Crain MR, Loes DJ, Greene GM, Ryals TJ, Sato Y. **MR imaging of cerebral ischemia: findings in the first 24 hours.** *AJNR Am J Neuroradiol* 1991;12:621-629
8. Moseley ME, Kucharczyk J, Mintorovich J, et al. **Diffusion-weighted MR imaging of acute stroke: correlation with T2-weighted and magnetic susceptibility-enhanced MR imaging in cats.** *AJNR Am J Neuroradiol* 1990;14:330-346
9. Mintorovich J, Moseley ME, Chaleuit L, et al. **Comparison of diffusion and T2-weighted MRI for the early detection of cerebral ischemia and reperfusion in rats.** *Magn Reson Med* 1991; 18:39-50
10. Moseley ME, Cohen Y, Mintorovich J, et al. **Early detection of regional cerebral ischemia in cats: comparison of diffusion and T2 weighted MRI and spectroscopy.** *Magn Reson Med* 1990; 14:330-346
11. van Gelderen P, de Vleeschouwer MHM, DesPres D, Pekar J, van Zijl PCM, Moonen CTW. **Water diffusion and acute stroke.** *Magn Reson Med* 1994;31:154-163
12. Warach S, Chien D LiW, Ronthal M, Edelman RR. **Fast magnetic resonance diffusion-weighted imaging of acute human stroke.** *Neurology* 1992;42:1717-1723
13. Warach S, Gaa J Siewert B, Wielopolski, Edelman RR. **Acute human stroke studies by whole brain echo planar diffusion-weighted magnetic resonance imaging.** *Ann Neurol* 1995;37: 231-241
14. Chien D, Kwong KK, Gress DR, Buonno FS, Buxon RB, Rosen BR. **MR diffusion imaging of cerebral infarction in humans.** *AJNR Am J Neuroradiol* 1992; 13:1097-1102
15. Le Bihan D, Turner R, Douek P, Patronas N. **Diffusion MR imaging: clinical applications** *AJR Am J Roentgenol* 1992; 13: 1097-1102
16. Marks MP, De Crespigny A, Lentz D, Enzmann D, Albers GW, Moseley ME. **Acute and chronic stroke: navigated spin-echo diffusion weighted magnetic resonance imaging.** *Radiology* 1996;199:403-408
17. Sorenson AG, Buononno FS, Gonzalez RG, et al. **Hyperacute stroke: evaluation with combined multisection diffusion-weighted and hemodynamically-weighted echo planar MR imaging.** *Radiology* 1996;199:391-401
18. Schlaug G, Siewert B, Benfield A, Edelman RR, Warach S. **Time course of the apparent diffusion coefficient abnormality in human stroke.** *Neurology* 1997;49:113-119
19. Welch KMA, Windham J, Knight RA, et al. **A model to predict the histopathology of human stroke using diffusion and T2 magnetic resonance imaging.** *Stroke* 1995;26:1983-1989
20. Le Bihan D. **Molecular diffusion magnetic resonance.** *Magn Reson Q* 1991;7:1-30
21. Beauchamp NJ, Aziz MU, Passe TJ, van Zijl PCM. **MR diffusion imaging in stroke: review and controversies.** *Radiographics* 1998; 18:1269-1283
22. Moseley ME, Sevick R, Wendland MF, et al. **Ultrafast magnetic resonance imaging: diffusion and perfusion.** *Journal of Canadian Association of Radiologists* 1991;42:31-38
23. Rother J, de Crespigny AJ, D'Arceuil H, Iwai K, Moseley ME. **Recovery of apparent diffusion coefficient after ischemia-induced spreading depression relates to cerebral perfusion gradient.** *Stroke* 1996;27:980-987
24. Norris DG, Niendorf T, Hoehn-Berlage M, Kohno K, Schneider EJ, et al. **Incidence of apparent restricted diffusion in three different models of cerebral infarction.** *Magn Reson Imaging* 1994;12:1175-1182

25. Loubinoux I, Volk A, Borredon J, Guirimand S, Tiffon B, Seylaz J, Meric P. **Spreading of vasogenic edema and cytotoxic edema assessed by quantitative diffusion and T2 magnetic resonance.** *Stroke* 1997;28:419-427
26. Leeds NE, Jackson EF. **Invited commentary accompanying reference 21.** *Radiographics* 1998;18:1283-1285
27. Edelstein WA, Bottomley PA, Hart HR, Smith LS. **Signal, noise, and contrasts in nuclear magnetic resonance (NMR) imaging.** *J Comput Assist Tomogr* 1983;7:391-401
28. Niendorf T, Dijkhuisen R, Norris D, Campagne M, Nicolay K. **Biexponential diffusion attenuation in various states of brain tissue: implications for diffusion-weighted imaging.** *Magn Reson Med* 1996;36:847-857
29. Tien Rd, Felsberg GJ, Friedman H, Brown M, Macfall J. **MR imaging of high-grade gliomas: value of diffusion-weighted echoplanar pulse sequences.** *AJR Am J Roentgenol* 1994;162:671-677
30. Tsuruda JS, Chew WM, Moseley ME, Norman D. **Diffusion-weighted MR imaging of the brain: value of differentiating between extraaxial cysts and epidermoid tumors.** *AJR Am J Roentgenol* 1990;155:1059-1065
31. Haimes A, Zimmerman R, Morgello S, et al. **MR imaging of brain abscesses.** *AJNR Am J Neuroradiol* 1989;10:279-291